ARED: Antibiotic Response determined by Euclidean Distance with highly sensitive Escherichia coli biosensors

Haoran Shi (haoran.shi13@alumni.xjtlu.edu.cn)
Xi'an Jiaotong-Liverpool University https://orcid.org/0000-0001-5997-6946

Trillion Surya Lioe
Xi'an Jiaotong-Liverpool University

Kelly van der Eng
Xi'an Jiaotong-Liverpool University

Ryanica Suryajaya
Xi'an Jiaotong-Liverpool University

Ziyi Feng
Xi'an Jiaotong-Liverpool University

Boris Tefsen
Ronin Institute: Ronin Institute for Independent Scholarship

Sam EV Linsen
Hangzhou SquaredAnt Network Technology Co Ltd

Research Article

Keywords: Bacterial biosensors, Antimicrobial resistance, Antibiotic sensitivity genes, Residue monitoring, Microbial Inhibition

Posted Date: November 5th, 2021

DOI: https://doi.org/10.21203/rs.3.rs-1013453/v1

Abstract

Antimicrobial Resistance is challenging healthcare and food security and is driven by antibiotic overuse and environmental pollution. Longitudinal monitoring of antibiotic residue would help to track pollution sources and assess the effect of interventions. Here we propose a novel high-throughput monitoring method. We mutagenized *E. coli* MG1655 and identified and characterized 12 antibiotic-sensitive biosensors (ABSBs) with different genotypes by a newly developed method called Antibiotic Response determined by Euclidean Distance (ARED), based on growth (OD_{600}) and metabolic activity (resazurin). The ABSBs contain nonsense or frameshift mutations in expected genes, like those coding for efflux pumps and lipopolysaccharide biosynthesis enzymes, as well as mutations in genes lesser or not known to be important for antibiotic sensitivity. Resazurin-based ARED can achieve antibiotic detection in the ng/mL range for most antibiotics tested in aqueous solutions. Our study shows that mutagenesis of *E. coli* can generate a tremendous shift in antibiotic sensitivity and that quantification of metabolic activity with ARED is a straightforward manner to monitor antibiotic activity in aqueous solutions. We propose that this method can be adopted for any collection of cell strains that possess differential antibiotic sensitivity and thus can be implemented for widespread monitoring of samples with unknown antibiotic complexion and origin.

Key Points

- ARED is a versatile antibiotic activity detection method
- Generation of 12 unique *E. coli* biosensors hypersensitive to antibiotics
- Suspected functional mutations in *pal* and *bamA* identified

Introduction

Antimicrobial resistance (AMR) greatly hinders the effectiveness of medical treatments, and has been one of the drivers of the re-emergence of several infectious diseases in recent years (Mulani et al. 2019; O'Neill 2014). Although the mechanisms of acquiring AMR vary (Reygaert 2018), a main driver is increased exposure of bacteria to antibiotics at sub-inhibitory level in humans (Llor and Bjerrum 2014), food animals (Van et al. 2020) and the environment (Rodriguez-Mozaz et al. 2020). Among these ecological niches, animal-based food has become one of the major sources of chronic exposure to low-dose antibiotics due to extensive prophylactic and therapeutic use in agricultural food production (Nüesch-Inderbinen et al. 2019; Shepherd and Jackson 2013; Wang et al. 2017).

To avoid chemical toxicity in food for human consumption, residue concentrations of individual veterinary pharmaceuticals and other chemical products are restricted by so-called maximum residue limits (MRLs) by, among others, the Food and Agriculture Organization of the United Nations (FAO) (FAO-WHO 2018), China (Guobiao standards 2019) and the EU (European Union Regulations Commission 2010). However, MRLs do not take into account the accumulation of different types of residues, and therefore disregard physiological interactions that can select for or against resistance (Baym et al. 2016). In addition, even when regulations are in place, the right analytical tools are often missing to implement these effectively (Ayukekbong et al. 2017; Founou et al. 2016). Recent findings of high concentrations of antibiotics in children in Hong Kong (Li et al. 2017) and Shanghai (Wang et al. 2018) further emphasize the need for alternative approaches to reduce the antibiotic footprint of the food industry.

One approach would be by enhanced monitoring and data openness to the public, which could drive a reduced antibiotic footprint of the food industry by creating market incentives and consumer involvement. Publicizing field data has been an important driver for resolving acid rain in Europe and the US in the 1990's (Grennfelt et al. 2020) and, more recently, has contributed to improved air quality in China (Kay et al. 2015). Antibiotic monitoring would be most effective near food production sites, as the environment in agricultural regions is constantly exposed to excreted or leaked antibiotics (Martinez 2009). For instance, the food animal biomass and antibiotic consumption in this industry in China are estimated to be 287 M tons (441M livestock units (LSU), where 1 LSU equals 650 kg) and 30,000 tons respectively (Bai et al. 2018; Schoenmakers 2020). Accordingly, the estimated antibiotic use is 100 ppm, the magnitude of which is consistent with a global estimate of antimicrobial consumption in food animals (Van Boeckel et al. 2015), while residue in food is normally detectable at ppb levels (Hassan et al. 2021).

Here, we introduce a new method called Antibiotic Response determined by Euclidean Distance (ARED) based on 12 antibiotic-sensitive biosensors (ABSBs), with each ABSB having its own specific antibiotic-sensitivity profile. Combined, these ABSBs,

generated based on *Escherichia coli* K12 strain MG1655 using random mutagenesis, can detect and separate different classes of antibiotics. Resazurin-based ARED enabled us to detect a number of antibiotics in a concentration range between 1.25 and 400 ng/mL (ppb). These concentrations overlap with MRL levels in food of many antibiotics, which are generally at the 1-100 ng/mL range, and are well below MRLs for tetracyclines and ciprofloxacin in milk. We demonstrate the application of this set of ABSBs in hierarchical clustering of tap water samples from different sources as a proof-of-principle. We expect that ARED-based methods can be further developed into cost-effective and easy to operate monitoring platforms.

Material And Methods

Bacterial Strains

The 12 ABSBs generated in this study were derived from *E. coli* K-12 MG1655, and named based on library number and position in the 384-well plate. The ABSBs will be abbreviated in the rest of the article for simplicity: SA03L04 (L4), SA19B14 (B14), SA21K01 (K1), SA25aC12 (C12), SA27H17 (H17), SA28I03 (I3), SA32A05 (A5), SA32N10 (N10), SA46C19 (C19), SA48C14 (C14), SA062A18 (A18), SA063F21 (F21). Strains generated in this study were deposited in China General Microbiological Culture Collection Center (CGMCC). *E. coli* GSO598 (Δ*acrB::kan*), *E. coli* GSO581 (Δ*tolC::kan*) and *E. coli* GSO231 (Δ*acrZ::kan*) (Hobbs et al. 2012) were used in this study as reference strains in the OD-based ARED.

The bacterial sequences were submitted to the NCBI website under BioProject PRJNA692079.

Culturing conditions and reagents

Typically, bacterial strains were grown in standard non-pH adjusted Luria-Bertani medium (LB) containing 1% tryptone, 1% NaCl and 0.5% yeast extract. In resazurin-based ARED, strains were cultured in medium containing 1% yeast extract and 0.5% NaCl. All strains were maintained on 1.5% LB agar in 9 cm petri dishes and stored in LB supplemented with 15% glycerol at -80°C. Reagents for growth media, antibiotics and resazurin sodium salt were purchased from Sigma-Aldrich, China. Antibiotics used in this study include ampicillin (AMP), chloramphenicol (CAM), ciprofloxacin (CIP), clarithromycin (CLA), doxycycline (DOX), erythromycin (ERY), norfloxacin (NOR), ofloxacin (OFX), oxytetracycline (OTC), rifampicin (RIF), sulfamethizole (SFZ), sulfamethoxazole (SFX), tetracycline (TET), trimethoprim (TMP), vancomycin (VAN).

UV mutagenesis

E. coli strains (MG1655 or B14) thawed from -80°C stocks were inoculated in LB, cultured in suspension shaking at 200 rpm for 4 hours at 37°C. OD_{600} of grown cultures was adjusted to 1, before being diluted 10,000-fold. These diluted suspensions (50 µL) were evenly spread on LB-agar petri dishes by glass beads. Directly after spreading, individual plates without lids were irradiated with 8,000 µJ/cm^2 UV-C light (254 nm) in a 30 seconds pre-heated CL-1000 UV cross-linker (Analytik Jena, US). Petri dishes were always placed at the same position within the chamber to ensure consistent UV exposure. A 100,000-fold dilution (50 µL) of the OD_{600} adjusted sample was plated out as non-irradiated control. Directly after irradiation, plated cells were incubated at 37°C for 16-18 hours, and colony forming units (CFU) from both UV-irradiated petri dishes (UVIP) and non-irradiated petri dishes (NIP) were counted to calculate survival rate (Nahrstedt and Meinhardt 2004) using the following formula:

Survival rate (%) = (CFU on UVIP * 10,000) / (CFU on NIP * 100,000) * 100

If the UVIP showed a survival rate of less than 5%, colonies were picked at random and grown for 16 to 18 hours in LB in a flat-bottom 384-well plate (Jet Biofil, China) to generate a Mutant Library Plate (MLP). The MLPs were either directly used to screen for antibiotic sensitivity or stored at 4°C for at most 7 days.

Antibiotic sensitivity screening to identify first- and second-generation ABSBs

Cell suspensions (1 µL) were taken from MLPs and inoculated in 75 µL LB (non-treated control), or LB supplemented with antibiotics in flat-bottom 384-well plates. Antibiotics were used in the following concentrations: 10 µg/mL ERY, 1 µg/mL TET when screening for first-generation ABSBs, and 2 µg/mL ERY, 2 µg/mL AMP, 2 µg/mL RIF, 200 µg/mL SFZ when screening for second-generation

ABSBs. Antibiotic screening plates were incubated at 37°C for 16 to 18 hours, and the inhibition of each strain was calculated based on the following equation:

Inhibition (%) = (OD_{600} of non-treated strain – OD_{600} of treated strain) / (OD_{600} of non-treated strain) * 100

Sensitive mutants were identified by an inhibition rate above 80% in the presence of antibiotic.

Sequencing and mutation identification

Illumina HiSeqTM paired-end sequencing was outsourced to Sangon (Shanghai, China) to obtain the whole genome sequences of 12 identified ABSBs and MG1655. The sequence data of all ABSBs has been deposited on NCBI BioProject (Accession number: PRJNA692079, see also section Bacterial Strains). The Sangon analysis pipeline included quality evaluation by FastQC (Andrews 2017) and adapter trimming by Trimmomatic (Bolger et al. 2014). It also included mapping against the MG1655 genome sequence on NCBI accession number NC_000913, sorting of alignments and duplicate identification using the BWA package (Li and Durbin 2009), SAMTools (Li et al. 2009) and Markduplicates (Broad Institute 2019), respectively. Output of the variation detection by Haplotype Caller (Van der Auwera et al. 2013) was adapted by removal of 1) loci with heterozygous annotation and 2) mutations where the maximal coverage across the ABSBs was less than 200 reads. All ABSBs combined harbored 166 mutations which were covered by a total of 40663 reads, with an average coverage of 245 (minimal 129, maximal 349) reads per mutation, compared to an overall coverage within the complete dataset of 272 (98% of coverage of our full dataset between lies between 199 and 398).

OD-based Antibiotic Response determined by Euclidean Distance (ARED)

For OD-based sensitivity assays, the OD_{600} of bacterial cultures was adjusted in LB to 0.1 before inoculation in LB supplemented with appropriate antibiotics in a flat-bottom 384-wells plate. Assays were performed in triplicate. The plates were sealed with optical film (Axigen), and incubated in a plate reader (BioTek Instrument, USA) for 13 hours at 37°C. Blank subtracted OD_{600} measurements were taken every hour. The plate was shaken at 200 rpm for 10 minutes prior to measurements. The Euclidean Distance (ED) was calculated over transformed data to enable comparisons independently of absolute intensity values. Data was transformed as follows: for each ABSB, the end-point OD_{600} value in non-treated sample was set to 100%, while the other OD_{600} values in both non-treated and antibiotic-treated samples were expressed as a fraction of 100%. ED was calculated based on the equation:

$$ED(p,q)=\sqrt{N}\sum_{i=1}(p_i-q_i)^2$$

N is the number of time points and $p_i q_i$ are the transformed OD_{600} values at each time point of respectively a non-treated and antibiotic-treated ABSB.

Resazurin-based ARED: plate design and handling

Non-coated 96-well plates (Jet Biofill) were filled with 10 µl of bacterial suspension at an OD_{600} of 0.1 in ultrapure water (UPW, obtained from a Milli-Q® IX water purification system), covered with parafilm, and stored at -80°C until use. To prevent differences caused by non-uniform temperature adaptation throughout a 96 well plate (the so-called edge-effect (Kim and Jang 2018)), the following plate handlings were done in a fixed order. Prior to adding medium, plates were kept on the bench at RT for 30 minutes. After adding 150 µL of medium by multichannel pipette, the plates were sealed (Axygen PCR-TS) gently shaken between the bench surface and fingers, and incubated for 4 hours in a 37°C stove. After incubation, plates were placed on ice immediately, and cooled for 10 minutes. Hereafter, the seal was removed from the plate, 10 µL of 0.2 mg/mL ice-cold resazurin was added, and the plate was half-immersed in a thin layer of water at ambient temperature, gently pushing the plate sideways and back, for 90 seconds. While keeping the plate at ambient temperature it was dried on a tissue and transferred to an imaging station.

Resazurin-based ARED: data collection and image analysis

The LED-illuminated imaging station had a USB digital camera (1080p camera with a 4.2 mm lens) that captured one image per minute of the plate via the Webcam Capture plugin (Jerome 2016) in ImageJ2 (Rueden et al. 2017) for at least 60 minutes. Of each time series, data of separate color channels was extracted and stored. RGB values were normalized (Finlayson et al. 1998) and the difference between the Red and Blue channel of the cell suspensions were calculated as a Metabolic Activity Indicator using the equation:

Metabolic Activity Indicator = (Red – Blue) / (Red + Blue + Green)

Data visualization and calculation of the ED was performed with the R package (R. Team 2014).

Resazurin-based ARED: data transformation for ED calculation

For each plate, the two most similar Metabolic Activity Indicator values out of the triplicate were selected to calculate the mean (referred to as weighted mean). Normalization was performed by subtracting negative controls' weighted mean values from the raw data at each corresponding time-point. Normalized values were then used to calculate the ED as described for the OD-based ARED. As the resazurin-based colorimetric approach occasionally led to higher intensity values in treated samples, we also calculated the linear distance (LD) as

$$LD(p,q) = {}_{N}\sum_{i=1}(p_i - q_i)$$

, where the plus or minus sign of ED is assigned to be consistent with the LD.

ARED: Data analysis and visualization

The ward.D2 method in the R package (R. Team 2014) was used for hierarchical clustering, after creating a table of the Pearson's r of among all ED values. Heatmaps were drawn using the gplots library (Warnes et al. 2016). In order to compare the cell ABSBs' hierarchical clustering alignment, we applied the dendextend package (Galili 2015), which also includes a non-parametric approach for the correlation between the aligned clusters. The *P* value of the clustering alignment was calculated through obtaining correlation values from randomizing our data 5000 times, and calculating the fraction of correlation values that were equal or larger than the one we observed in our non-randomized data. Graphs and plots of data collections were made in LibreOffice (The Document Foundation 2020), the R package (R. Team 2014) and optimized with Inkscape (Inkscape Project 2020).

Tap water sampling

Tap water samples were collected from the laboratory and a household in Suzhou, China and from households in three municipalities in North-Holland, the Netherlands. Tap water was run consistently for 30 seconds and then 40 mL was collected in a 50 mL Falcon tube or PET bottle. Samples were diluted 2-fold in UPW and assessed directly by ARED or stored at 4°C for later use. Resazurin-based ARED of tap water samples was performed either in an imaging station as described above or in a Varioskan Lux multimode microplate reader (ThermoFisher Scientific, USA) with 560 nm excitation/590 nm emission.

Results

Selection of first-generation ABSBs

To generate a set of ABSBs with hypersensitivity to different antibiotics, UV irradiation was chosen as an unbiased mutagenic approach. Appropriate antibiotics for sensitivity screening were selected from the Antibiotic Residue Index (ARI), a comprehensive overview of antibiotic residue in the environment (Linsen 2021). In the initial screen, two widely used antibiotics, TET (listed #1 in the ARI) and ERY (listed #7 in the ARI) were selected.

In total 7392 mutants were screened for increased sensitivity to 1 µg/mL TET and 10 µg/mL ERY by checking the endpoint growth inhibition in LB. These concentrations have been shown to not impair growth of MG1655 (Hobbs et al. 2012) and this was confirmed through our experiments. Three ABSBs (B14, K1, L4) displayed growth inhibition greater than 80% for at least one of these antibiotics (Fig. 1a), and whole-genome sequencing of these ABSBs revealed seven different mutations across six different genes (Table 1) and five mutations in genomic regions lacking annotation (Table S1).

Table 1
Mutated genes in first generation ABSBs derived from MG1655

ABSB	Nonsense	Frameshift	Missense
B14	-	*acrB* (Leu25fs)	*agaS* (Pro223Leu), *cysJ* (Pro490Ser), *djlA* (Leu14Ser), *yhiN* (Glu355Lys)
K1	-	*gmhA* (Phe97fs)	-
L4	*acrB* (Gln577*)	-	-

One frameshift mutation in B14 and one nonsense mutation in L4 were both predicted to result in the lack of AcrB, an essential part of the AcrAB-TolC drug efflux pump (Du et al. 2014). Consistent with previous reports that AcrAB-TolC is responsible for the clearance of TET and ERY (Nolivos et al. 2019; Stubbings et al. 2005), B14 and L4 exhibited hypersensitivity to these two antibiotics (with growth inhibition ranging from 77–97%). The mutation in *gmhA* in K1 should compromise the outer membrane (OM) of this ABSB, as GmhA is crucial for the synthesis of heptose in LPS, the absence of which has been shown to increase bacterial sensitivity to hydrophobic antibiotics (Raetz and Whitfield 2002; Taylor et al. 2008). Indeed, enhanced entry of hydrophobic molecules such as ERY was apparent in K1, with a growth inhibition of 97%, while the permeability towards TET, a hydrophilic molecule, was much less affected in this ABSB (only 15% growth inhibition) compared to B14 and L4.

Second-generation ABSBs

While three ABSBs had been successfully created, to enable testing of a wide range of antibiotics more ABSBs with diversified sensitivities would have to be generated. We used B14 as the parent strain for a second-round screening, as this ABSB possesses four missense mutations, of which three (in *cysJ*, *djlA*, and *yhiN*) potentially contribute to antibiotic sensitivity (Clarke et al. 1996; Liu et al. 2019; Mitosch et al. 2017); see Table S2 for more background on these genes. To select ABSBs with diversified sensitivities, four antibiotics with different modes of action were used in this screening, namely ERY, AMP (listed #2 in the ARI), RIF (listed #12 in the ARI), and SFZ (listed #60 in the ARI). Amongst 9642 second-generation mutants, nine ABSBs were identified with enhanced sensitivity to at least one of these antibiotics (Fig. 1b).

Sequencing of the second-generation ABSBs revealed mutations in 34 genes in addition to those already present in parent strain B14 (Table 2) as well as mutations in 24 non-annotated regions (Table S1)

Table 2
Additional mutated genes in second-generation ABSBs derived from B14

ABSB	Nonsense	Frameshift	Missense
A5	*sapA* (Lys117*)	-	*lldP* (Phe531Ser), *mdtC* (Lys287Ile), *murJ* (Ala63Thr), *rem* (Gly72Glu), *ybeF* (Gln164His)
A18	*lpxM* (Trp203*)	-	*idnO* (Lys197Arg), *ogrK* (Ala37Val), *uvrC* (Val296Ile), *yjbL* (Lys226Asn), *yjbS* (Tyr35Cys)
C12	-	-	*nrdF* (Met97Ile), *oppF* (Gly7Arg), *pal* (Leu133Pro), *rsmG* (Pro88Ser), *yjfC* (Gly317Asp)
C14	*yaaA* (Leu28*)	-	*bamA* (Ser502Phe), *trkG* (Leu205Pro), *wbbI* (Ile25Asn)
C19	*yaaA* (Leu28*)	*ldtF* (Leu25fs)	-
F21	*waaG* (Leu298*)	-	-
H17	*yaaA* (Leu28*)	*tolB* (Lys2fs)	*appY* (Leu184Arg)
I3	-	*waaF* (Phe98fs)	*ydhV* (Arg677Cys)
N10	*tolA* (Lys309*)	-	*ddpD* (Pro144Ser), *frdA* (Arg107Ser), *kefF* (Leu35Phe), *purT* (Pro236Ser), *thiH* (Glu295Lys), *yhdP* (Gly1208Asn)

Eight of the identified nonsense, frameshift and missense mutations are in genes important for cell envelope integrity, i.e. in the Tol-Pal complex, OM to peptidoglycan tethering and LPS synthesis. (*bamA*, *ldtF*, *lpxM*, *pal, tolA*, *tolB*, *waaF*, *waaG*) (Bennion et al. 2010; Clementz et al. 1997; Morè et al. 2019; Szczepaniak et al. 2020; Werner and Misra 2005; Yethon et al. 2000).

The Tol-Pal complex is known to help maintain cell envelope integrity in Gram-negative bacteria and a lack of any of its functional components will result in enhanced entry of several antibiotics (Szczepaniak et al. 2020). H17 has a defective TolB caused by early frameshift mutations on position 2 and N10 has a nonsense mutation in *tolA* leading to a stop codon at position 309. Interestingly, C12 has a missense mutation leading to a change of the leucine at position 133 in Peptidogylcan Associated Lipoprotein (Pal). This leucine is highly conserved among many Gram-negative bacteria and part of a domain that is important for binding to TolB and peptidoglycan (Cascales and Lloubès 2004).

Disruption of OM to peptidoglycan tethering is expected to weaken the cell envelope, and thus a reduced barrier for antibiotics to reach their target. The frameshift mutation in *ldtF* in C19 leads to a truncated version of the protein LdtF, a recently identified L,D-endopeptidase. LdtF has been shown to cleave the cross-links between peptidoglycan and Braun's lipoprotein, thereby disturbing the tethering of the OM to peptidoglycan (Bahadur et al. 2021). The *bamA* missense mutation in C14 could lead to diminished assembly of β-barrel proteins, including TolC, directly (Werner and Misra 2005), or indirectly (Bennion et al. 2010). Interestingly, systematic linker scanning mutagenesis of b*amA* showed that a change in residues 503 and 504 lead to lethality or increased sensitivity towards VAN, respectively (Browning et al. 2013). The mutation identified in C14 involves the directly adjacent serine at 502 into a phenylalanine; a change that could very well disrupt proper folding of β-strand β6 and thus compromise barrel formation essential for functioning of BamA. Indeed, C14 shows the highest sensitivity to 250 ng/mL VAN (Table 4).

Table 4
ED values for ABSBs and control strain from resazurin-based ARED

Antibiotic (ng/ml)	MG1655[a]	A5	A18	B14	C12	C14	C19	F21	H17	I3	K1	L4	N10
AMP 400	0.4	0.9	1.4	0.5	**4.0 G**	0.4	0.0	0.6	**3.9 G**	1.1	**2.1**	1.0	**2.3 G**
CAM 100	0.7	**2.3 G**	**2.1 G**	1.9	1.9	**2.1 G**	**3.2 G**	**2.9 G**	**2.2 G**	**3.2 G**	1.3	**3.0**	0.6
CIP 1.25	1.3	**3.3 G**	**3.5 G**	1.9	0.3	**2.2 G**	1.8	**2.5 G**	2.0	**2.8 G**	0.5	1.8	-1.8
CLA 500	0.5	**2.2 G**	**2.2 G**	1.2	**3.4 G**	**3.0 G**	**2.2 G**	**2.8 G**	**2.7 G**	**4.7 G**	**5.0**	1.4	1.8
DOX 50	1.1	**4.6**	**4.9**	**5.2**	**4.4**	**6.2**	**5.6**	**6.3**	**4.3**	**5.8**	**5.0**	**5.7**	**3.5**
NOR 15	0.9	**4.5**	**4.9**	**3.8**	**2.1**	**4.6**	**3.1**	**3.6**	**2.5**	**3.7**	**2.7**	**2.5**	-0.6 L
OFX 25	0.6	**5.0**	**5.1**	**5.0**	**3.6**	**5.4**	**5.3**	**6.0**	**4.0**	**4.9**	**2.5**	**5.4**	**3.6**
OTC 50	1.5	**3.4**	**3.7**	**4.2**	**2.4**	**4.8**	**3.8**	**3.9**	**2.8**	**3.6**	**2.8**	**4.9**	**2.9**
RIF 50	1.0	0.5	**2.9 G**	0.8	**2.4 G**	0.0	**2.6 G**	-0.7	2.0	**6 G**	**5.3**	-0.6	1.6
TET 25	0.6	**3.3**	**2.4**	**3.5**	**2.3**	**3.7**	**3.0**	**2.9**	**2.9**	**2.2**	2.0	**2.9**	1.2 L
TMP 20	1.4	**2.1 G**	1.3	1.7	0.8	**2.3 G**	1.8	1.9	0.9	1.9	**2.9**	**2.6**	1.2
VAN 250	0.8	**3.5**	**2.2**	**2.5**	-0.7 L	**3.8**	-0.4 L	-0.4 L	-1.4 L	-0.7 L	-0.6	0.8	-1.5 L

[a]Mean values from 15 replicates for MG1655 and from triplicates for other ABSBs. The average standard deviation within this dataset was 0.47. Values above the threshold of 2.03 are in bold; a 'G' or 'L' behind a value indicates a gain or loss, respectively, of sensitivity in this ABSB compared to its mother strain B14.

Defective lipopolysaccharide (LPS) synthesis will lead to a compromised OM (Ebbensgaard et al. 2018; Raetz and Whitfield 2002). Second-generation ABSB A18 has a premature stop codon at position 203 in LpxM, the myristoyltransferase responsible for adding the final secondary acyl chain to generate hexa-acylated lipid A, the hydrophobic moiety of LPS embedded in the OM (Clementz et al. 1997), while I3 has a frameshift mutation causing a premature stop codon after 129 amino acids and thus a defective WaaF, the heptosyltransferase that adds the last heptose to the inner saccharide core of LPS (Ebbensgaard et al. 2018; Yethon et al. 2000).

F21 has a premature stop at position 298 in WaaG, the glucosyltransferase adding the first glucose to the inner saccharide core of LPS (Yethon et al. 2000).

The role of SapA in antibiotic sensitivity is less evident from literature. It seems an interesting candidate for further study, backed by the presence of a nonsense mutation in its gene in A5 and leads obtained from literature. SapA is predicted to be periplasmic and was shown to be important for resistance of *H. influenzae* to antimicrobial peptides (Mason et al. 2005). Not much is known about its function in *E. coli* yet, but it might help in stabilizing cell envelope integrity or efflux of certain molecules from the cytoplasm by interacting with the putrescine exporter SapBCDF (Sugiyama et al. 2016). Furthermore, it was shown that a SapA deletion mutant had enhanced accumulation of the cationic fluorescent dye carbocyanine diS-C3(5) (Jindal et al. 2019) and it is upregulated upon TET and TMP exposure (Mitosch et al. 2017), indicating a potential role for SapA in the efflux of certain antibiotics.

Lastly, attention needs to be given to *yaaA*, as an identical nonsense mutation in this gene was identified in three ABSBs (C14, C19 and H17). We reasoned that this allele must have originated from a hybrid population of parent strain B14 during the mutagenesis procedure. Indeed, our sequencing data revealed two alleles at two positions, one in the *yaaA* gene at position 6377 (covered by 136 reads with the reference sequence and 68 reads with the mutation) and one in an undefined genomic region at position 2025279 (covered by 77 reads with the reference sequence and 149 reads with the mutation), which were mutually exclusive in the B14-derived strains. The origin of these two mutations is very interesting, but discussing the impact on antibiotics would be speculative, from which we refrain in this report.

Antibiotic sensitivity profiling using OD-based ARED

Diverse antibiotic sensitivities are expected in the set of 12 ABSBs due to their varied genotype. To fully utilize the potential of these ABSBs as biosensors, reference profiles of antibiotic sensitivity are useful for comparison with test results from field samples to deduce the presence of potential antibiotics. In addition to four antibiotics used in the screening (AMP, ERY, RIF, TET), CIP (listed #3 in the ARI), CAM (listed #4 in the ARI), TMP (listed #6 in the ARI), DOX (listed #14 in the ARI), OTC (listed #17 in the ARI), and SFX (listed #5 in the ARI) were further included for profiling. To generate a quantitative antibiotic sensitivity profile for each ABSB, we developed a novel method called Antibiotic Response determined by Euclidean Distance (ARED). OD-based ARED compares treated sample with non-treated control by calculating Euclidean distance (ED) using transformed OD_{600} measurements from all time points (Fig. 2a). This method is expected to reveal subtle strain-specific growth characteristics that are not picked up using endpoint growth assays.

Table 3
ED values for ABSBs and control strains in OD-based ARED with ten different antibiotics

Antibiotic (ng/ml)	MG 1655[a]	GSO 231	GSO 581	GSO 598	A5	A18	B14	C12	C14	C19	F21	H17	I3	K1	L4	N10
AMP 1000	0.2	0.2	0.1	0.1	0.1	0.1	0.3	**0.9 G**	0.2	0.2	0.2	**1.1 G**	0.4	0.1	0.1	**1.3 G**
CAM 250	0.4	0.3	**0.8**	**0.7**	**0.8**	**0.9**	**0.9**	**1.0**	**1.0**	**1.0**	**0.7**	**1.0**	**0.9**	0.4	**0.9**	**1.0**
CIP 2.5	0.2	0.3	**1.0**	**0.8**	**0.7**	0.6 L	**1.2**	**1.2**	**1.0**	0.6 L	**0.8**	**1.1**	**0.7**	0.3	**0.8**	0.7 L
DOX 250	0.3	0.3	**1.1**	**1.1**	**1.2**	**1.3**	**1.2**	**1.0**	**1.4**	**1.5**	**1.3**	**1.2**	**1.7**	**0.9**	**1.3**	**1.1**
ERY 1000	0.2	0.2	0.6	0.2	0.1	0.5	0.3	0.3	**0.9 G**	0.3	0.5	0.6	**1.1 G**	0.7	0.2	**0.7 G**
OTC 250	0.3	0.6	0.5	0.7	**0.8**	**0.7**	**0.9**	0.7 L	**0.7**	**0.8**	0.4 L	0.7 L	0.6 L	0.2	**1.0**	0.7 L
RIF 1000	0.2	0.2	0.1	0.2	0.2	0.2	0.4	0.5	0.5	0.2	0.1	0.6	**1.1 G**	**1.8**	0.3	0.6
SFX 200000	0.3	0.4	0.3	0.3	0.3	0.3	0.6	0.6	0.3	0.4	0.2	0.6	**0.9 G**	0.5	0.5	0.4
TET 500	0.6	0.6	**0.8**	**1.0**	**1.0**	**1.1**	**1.1**	**1.2**	**1.2**	**1.2**	**1.0**	**1.2**	**0.7**	0.1	**1.1**	**1.1**
TMP 25	0.2	0.3	0.3	0.6	**1.0**	0.6 L	**0.9**	**0.7**	**0.7**	0.6 L	0.4 L	0.6 L	0.6 L	0.3	**0.8**	**1.0**

[a]Mean values from 15 replicates for MG1655 and from triplicates for other strains. The average standard deviation within this dataset was 0.05. Values above the threshold of 0.69 are in bold; a 'G' or 'L' behind a value indicates a gain or loss, respectively, of sensitivity in this ABSB compared to its mother strain B14.

We determined ED values for each strain and antibiotic, and an ABSB was considered to have enhanced sensitivity if its ED value was higher than 0.69 (3 standard deviations above the MG1655 mean). Accordingly, the minimal concentrations of the profiled antibiotics where one or more ABSBs show enhanced sensitivity were identified (Table 3). We also compared the distributions of aggregated EDs from the 12 ABSBs with those from MG1655 and GSO strains (Fig. 2b). The difference between the ED distribution of MG1655 and ABSBs was statistically significant using a two-sample Wilcoxon test ($P_{Wilcoxon}$ = 8.35e-12), indicating an increase in overall sensitivity towards this set of antibiotics. GSO strains harboring mutations in AcrAB-TolC efflux pump have been shown to exhibit hypersensitivity to antibiotics (Hobbs et al. 2012), and the profiles of Δ*acrB* strain GSO598 and Δ*tolC* strain GSO581 indeed showed significant similarity to the ABSBs ($P_{Wilcoxon}$ = 0.11). GSO581 and GSO598 display quite similar phenotypes, with quantitatively comparable enhanced sensitivity towards most antibiotics, with TET 500 being the only exception for which loss of AcrB caused a stronger phenotype than loss of TolC. In contrast, *ΔacrZ* strain GSO231 was not more sensitive than MG1655 towards most of the antibiotics tested at these concentrations, except for OTC and CIP.

To visualize similarities and differences between the strains tested in this way, we performed hierarchical clustering based on the calculated correlations between the ED values for each antibiotic and strain (Fig. 2c). Evidently, each strain displays a different antibiotic sensitivity profile, with the deep red squares indicating the highest sensitivity. MG1655 and GSO231, the two least sensitive strains we tested, form a cluster that is clearly separated from all ABSBs and the two other GSO strains. GSO598 clusters with B14 and L4, the first-generation ABSBs which also lack a functional AcrB. Furthermore, GSO581 clusters with F21 and C14, which is expected to have a disrupted TolC assembly due to the mutation in *bamA*. Together, these observations illustrate the potential of OD-based ARED to differentiate between antibiotic-sensitive strains with different genotypes.

Resazurin-based ARED

OD-based approaches for antibiotic detection are relatively time consuming, and the first few hours in such methods are the least informative as hardly any detectable changes in OD are provided (Choi et al. 2014), although effects of antibiotics on bacteria already emerge soon after exposure (Mitosch et al. 2017; Stubbings et al. 2005). The highly sensitive redox indicator resazurin is

commonly used for measuring metabolic activity as an indicator for the number of viable cells, for instance in an early study measuring the response of *M. tuberculosis* to antimicrobials (Yajko et al. 1995). We modified the OD-based ARED using resazurin and subjected the set of ABSBs to the colorimetric approach dubbed resazurin-based ARED, which is expected to provide a more sensitive response to antibiotics in a shorter time-frame. A typical signal response with and without 50 ng/mL RIF is shown for K1 (Fig. 3a), to illustrate that differences already become apparent within 10 minutes.

Overall, the sensitivity of the ABSBs to 12 antibiotics was determined using resazurin-based ARED. Out of these antibiotics, eight were used previously (AMP, CAM, CIP, DOX, OTC, RIF, TET and TMP), and newly added were OFX (listed #9 in the ARI), CLA (#25 in the ARI), NOR (#18 in the ARI) and VAN (not in the ARI). The aggregated ED values for MG1655 exposed to all antibiotics for 60 minutes significantly differed from those of the 12 ABSBs ($P_{Wilcoxon}$ = 0.00012) (Fig. 3b), in line with the results obtained with OD-based ARED. On top of being a faster method, it also enabled to measure inhibitory effects at concentrations up to 20-fold lower than those for corresponding antibiotics in OD-based ARED (Table 4). An ABSB was considered to have enhanced sensitivity if its ED value was higher than 2.03 (3 standard deviations above the MG1655 mean) for the conditions shown in Table 4.

Similar to the OD-based ARED, we performed hierarchical clustering to visualize the correlations of the ED values between all strains. Two distinctive main clusters can be seen, with the first, consisting of C12, H17, I3, K1 and N10 strongly responding to AMP, RIF and/or CLA, while the second cluster, consisting of A18, C14, B14, A5, C19, F21 and L4 is more sensitive to CAM, tetracyclines, quinolones and VAN (Fig. 3c). In Table S2 we elaborate on the observed phenotypes of the ABSBs in light of the mutants on annotated genes in *E. coli*.

We were also interested to see to what extent B14-derived ABSBs gained or lost sensitivity according to our set thresholds in the two assays. In OD-based ARED, B14 showed sensitivity to six antibiotics, five B14-derived ABSBs gained sensitivity to at least one of the four remaining antibiotics. In resazurin-based ARED, B14 also showed sensitivity to six antibiotics, and all nine B14-derived ABSBs gained sensitivity to at least one of the other six antibiotics. However, we also observed loss of sensitivity in B14-derived strains in both approaches, most prominently OD-based ARED in presence of CIP, OTC, and TMP; sensitivity loss is observed in both assays in the ABSBs C12, N10, H17, C19, F21 and I3 and (Table 3, 4). Whether or not mutations in this complex would alter the response to antibiotics in the B14 background would require further study.

The correlation analysis and hierarchical clustering analysis shown in Figs. 2c and 3c provide an overview of the responses measured in both methods. A comparison of these two outcomes could elucidate the presence or absence of method-induced biases. To this end we aligned dendrograms of ABSBs that were exposed to the same antibiotic in both OD-based ARED and resazurin-based ARED (Fig. 4a), using the R library dendextend (Galili 2015). The similarities in branching lead to a non-parametric correlation of 0.76 (P = 0.065), indicating a reasonable positive relation in the response of ABSBs. Comparing the dendrograms for both methods, but now for each strain tested, shows that seven out of the 13 strains are in identical subbranches originating from a common node (Fig. 4b). With a correlation of 0.8 (P = 0), the antibiotics evoke a response that is fairly consistent across the two methods. The identical clustering of C12, H17 and N10 in both OD- and resazurin-based ARED seems to be mainly caused by the strong response that these three ABSBs exhibit to AMP. Also, they all have mutations in one of the components of the TolAB-Pal complex, which is known to result in a classical periplasmic leakage phenotype (Kern et al. 2019). Both K1 and I3 carry mutations in the heptose biosynthesis pathway. K1 does not synthesize heptose in LPS and I3 cannot transfer heptose to LPS, thus these two ABSBs fall into one cluster as expected. Given that these alignments show a good positive correlation, we conclude that the methods themselves have only a mild effect on the results, and hierarchical clustering is an effective tool to align the ED values. Altogether, both ARED approaches can be informative for investigating antibiotics in aqueous samples. Resazurin-based ARED detects responses at lower antibiotic concentrations and can better discriminate the response of B14 and its derived ABSBs than OD-based ARED.

Antibiotic assessments in tap water

The analysis of the ED values from OD- and resazurin-based ARED shows that specific responses can be explained by the genetic background of the ABSBs, and that strains with different mutations in overlapping pathways show similar responses. We therefore expect that an assay based on a set of ABSBs can also discriminate between samples with an unknown composition. Here, we tested our ABSBs on tap water samples collected from Suzhou (China) and three cities in the Netherlands. To address the impact of antibiotics on tap water results, we also included one tap water sample supplemented with RFP (50 ng/mL). Tap water in these

regions is routinely monitored and quality indicators are shared publicly (Hua Yan Water 2021; Waternet 2021). Depending on the water source and the sanitizing methods applied, tap water may vary in composition with respect to minerals, sanitizing residue, and redox potential, which may influence cell growth, and, in case of resazurin-based ARED, may affect staining itself. Tap water samples did not inhibit the OD-based growth of MG1655 and ABSBs (data not shown). We then investigated whether resazurin-based ARED would be sensitive to non-antibiotic compounds that could be present in tap water samples. We tested individually against the metals zinc (0.5 to 1 µg/mL) and lead (5 to 20 ng/mL), as well as chlorine (0.5 to 50 µg/mL), and did not find a negative effect (data not shown). However, in our resazurin-based ARED, we found that compared to UPW, tap water did delay staining, including in samples without cells (Fig. 5a). This delay also had a large impact on the ED of MG1655 (Fig. 5b), which should be around 0 but increased in value in tap water samples. Since we did not have a “control tap water” sample and we had to use UPW as a reference, we sought an alternative approach to deal with the delay in staining and decided to subtract the MG1655 ED from all ABSBs ED values. By hierarchical clustering of these positive-control subtracted values, the samples clustered well according to our sampling locations: two main branches were formed, with the largest one including tap water samples from the Netherlands (Bloemendaal, Amsterdam and Driehuis) in one subbranch, and the two samples from Suzhou in another subbranch. The second main branch contained only one sample: the Suzhou tap water sample supplemented with RIF (50 ng/mL) (Fig. 5c). Taken together, this analysis shows that the resazurin-based ARED method is sensitive for sample types, which needs to be addressed when further developing this method as a monitoring tool. We observed that ABSBs respond differently to RIF dissolved in tap water compared to RIF in UPW. For instance, I3 hardly responds in tap water, while it strongly responds to RIF in UPW (Fig. 3c). In spite of this discrepancy in the responses of individual ABSBs, the presence of the antibiotic can still be revealed by the response of all ABSBs collectively.

Discussion

Bacteria in suspension have been long used as antibiotic sensors in commercial applications, especially the multi-sensitive *G. stearothermophilus* var. calidolactis. These have been integrated in microbial inhibition assays developed for the dairy industry (Navrátilová 2008), where growth is detected by a pH indicator. A current shortcoming of these commercialized microbial inhibition assays is the lack of identification information following a positive result: they only lead to a conclusion on presence or absence of antibiotic activity. In the present study, we offer a potential solution for this shortcoming by including multiple ABSBs with diversified sensitivities, while consolidating the ED of colorimetric (resazurin-based ARED) or optical density (OD-based ARED) data over multiple time points. As we have shown, ARED allows us to measure the impact of multiple antibiotics at concentrations down to the ng/mL level, and the hierarchical clustering of ABSBs that are exposed to the same group of antibiotics correlates well across the two methods. Together, the application of ABSBs in the ARED assay could be useful in antibiotic detection, and simultaneously provide indications for identification. This would be useful in situations where the antibiotic complexion of samples may be diverse and antibiotic identification is needed for tracking a pollution source.

In this study, we have generated 12 biosensors with enhanced antibiotic sensitivity from wild type *E. coli* K-12 MG1655 using UV mutagenesis. The motivation to use *E. coli* was a pragmatic one, as it is a resource-rich, versatile model system which has been applied in antibiotic detection before (Liu et al. 2010). In these ABSBs, several nonsense and frameshift mutations in genes responsible for cell envelope synthesis or efflux pumps could be linked to the antibiotic sensitivity profile of the individual ABSBs. For a few of the mutations this was not obvious, not from literature, nor from our data, and it was beyond the scope of this study to further investigate a potential role in antibiotic sensitivity of those genes further. Clearly, identification of new genes that could be targeted to increase antibiotic sensitivity could be exploited in the fight against antibiotic resistant pathogens (Ayhan et al. 2016).

The detection limit of resazurin-based ARED is in the ng/mL range and thus approaching that of analytical chemistry methods (Munteanu et al. 2018); the rate-limiting factor being the sensitivity of the ABSBs that we identified in this study. A number of practical challenges still need attention, as shown in the tap water analysis. This, in our view, does not disqualify the application of ABSBs to detect antibiotic residue by this method, but rather points in the direction how to optimize the method further. Essential considerations include: which reference sample is used along which the ED is calculated? How to align the positive control (in our case, MG1655) data for the reference sample and test sample? How to control for redox potential in samples that could influence resazurin staining? Such questions could be addressed by setting boundaries for the negative and positive controls; and, as we did here, dilution of samples in UPW and subtracting the positive control; additionally, the construction of a standard reference sample by mixing test samples could also be useful to look for deviations in the response of ABSBs. Another challenge is that correlation

alone is incomplete without descriptive insights on the raw data. A dashboard consisting of a combination of Figs. 5a and 5c would visualize the data from these two angles.

Resazurin-based ARED could be used for commercial applications, by combining a proper set of ABSBs and integrating a tool to obtain colorimetric data over multiple time points. To enable this, we are currently optimizing a novel device, where ABSBs are stored on isolated pieces of non-woven polyester fabric that is sealed off from an absorptive matrix for fluid absorption. Under a second seal, patches of dried-up resazurin solution are placed. By introducing medium onto the absorptive matrix, and removing the seal, ABSBs will be exposed to medium, and cell propagation can then initiate. Staining can be achieved after breaking the second seal between the absorptive matrix and the resazurin patch (Linsen 2020). This method would allow for simple storage, handling and readout without the need of laboratory equipment and thus be interesting for use as a consumer product.

In conclusion, ARED based on multiple ABSBs can successfully detect antibiotics in solution. The application of this method in monitoring antibiotic pollution could lead to improvements of existing microbial inhibition assays, especially in samples for which *a priori* knowledge on the antibiotic types or pollution sources is lacking.

Declarations

Acknowledgments

We sincerely thank Jolien Snellen for collecting tap water samples in the Netherlands and Jessica Linsen-Cao for general support. We are also thankful to Jan Tommassen (Utrecht University) and Gisela Storz (NIH, Bethesda) for providing MG1655 and the GSO strains, respectively.

Author's contribution

BT, and SL were involved in the conception and research design. HS, TSL, ZF, RS, KvdE and SL conducted experiments. HS, BT and SL analyzed the data, and wrote the manuscript. All authors read and approved the manuscript.

Funding Information

This work was funded by SquaredAnt and the Key Programme Special Fund from the Suzhou Dushu Lake Science and Education Innovation District Administrative Committee (SEIDAC), Suzhou Industrial Park Science & Technology and Information Bureau (STIB) and XJTLU (Grant No. KSF-E-09).

Availability of data and material

The dataset used and/or analyzed during the current study are available from the corresponding authors on reasonable request.

Code availability

Available on GitHub (https://github.com/mmrmas/supplementsARED).

Conflict of interest

Sam Linsen is the founder and owner of [redacted] (SquaredAnt). The findings described in this paper are the result of a collaborative project between the university XJTLU and this company.

Ethical approval

This article does not contain any studies with human participants or animals performed by any of the authors.

References

Andrews S (2010) FastQC: a quality control tool for high throughput sequence data.

Ayhan DH, Tamer YT, Akbar M, Bailey SM, Wong M, Daly SM, Greenberg DE, Toprak E (2016) Sequence-Specific Targeting of Bacterial Resistance Genes Increases Antibiotic Efficacy. PLoS Biol 14(9):e1002552. doi:10.1371/journal.pbio.1002552

Ayukekbong JA, Ntemgwa M, Atabe AN (2017) The threat of antimicrobial resistance in developing countries: causes and control strategies. Antimicrob Resist Infect Control 6:47. doi:10.1186/s13756-017-0208-x

Bahadur R, Chodisetti PK, Reddy M (2021) Cleavage of Braun's lipoprotein Lpp from the bacterial peptidoglycan by a paralog of l,d-transpeptidases, LdtF. Proc Natl Acad Sci U S A 118(19). doi:10.1073/pnas.2101989118

Bai Z, Ma W, Ma L, Velthof G, Wei Z, HavlÌk P, Oenema O, Lee MR, Zhang F (2018) China s livestock transition: Driving forces, impacts, and consequences. Sci Adv 4(7):eaar8534. doi: 10.1126/sciadv.aar8534

Baym M, Stone LK, Kishony R (2016) Multidrug evolutionary strategies to reverse antibiotic resistance. Science 351(6268):aad3292. doi:10.1126/science.aad3292

Bennion D, Charlson ES, Coon E, Misra R (2010) Dissection of β-barrel outer membrane protein assembly pathways through characterizing BamA POTRA 1 mutants of Escherichia coli. Mol Microbiol 77(5):1153-71. doi:10.1111/j.1365-2958.2010.07280.x

Bolger AM, Lohse M, Usadel B (2014) Trimmomatic: a flexible trimmer for Illumina sequence data. Bioinformatics 30(15):2114-20. doi:10.1093/bioinformatics/btu170

Broad Institute (2019) Picard toolkit. Broad Institute, GitHub repository

Browning DF, Matthews SA, Rossiter AE, Sevastsyanovich YR, Jeeves M, Mason JL, Wells TJ, Wardius CA, Knowles TJ, Cunningham AF, Bavro VN, Overduin M, Henderson IR (2013) Mutational and topological analysis of the Escherichia coli BamA protein. PLoS One 8(12):e84512. doi:10.1371/journal.pone.0084512

Cascales E, Lloubès R (2004) Deletion analyses of the peptidoglycan-associated lipoprotein Pal reveals three independent binding sequences including a TolA box. Mol Microbiol 51(3):873-85. doi:10.1046/j.1365-2958.2003.03881.x

Choi J, Yoo J, Lee M, Kim EG, Lee JS, Lee S, Joo S, Song SH, Kim EC, Lee JC, Kim HC, Jung YG, Kwon S (2014) A rapid antimicrobial susceptibility test based on single-cell morphological analysis. Sci Transl Med 6(267):267ra174. doi:10.1126/scitranslmed.3009650

Clarke DJ, Jacq A, Holland IB (1996) A novel DnaJ-like protein in Escherichia coli inserts into the cytoplasmic membrane with a type III topology. Mol Microbiol 20(6):1273-86. doi:10.1111/j.1365-2958.1996.tb02646.x

Clementz T, Zhou Z, Raetz CR (1997) Function of the Escherichia coli msbB gene, a multicopy suppressor of htrB knockouts, in the acylation of lipid A. Acylation by MsbB follows laurate incorporation by HtrB. J Biol Chem 272(16):10353-60. doi:10.1074/jbc.272.16.10353

Du D, Wang Z, James NR, Voss JE, Klimont E, Ohene-Agyei T, Venter H, Chiu W, Luisi BF (2014) Structure of the AcrAB-TolC multidrug efflux pump. Nature 509(7501):512-5. doi:10.1038/nature13205

Ebbensgaard A, Mordhorst H, Aarestrup FM, Hansen EB (2018) The Role of Outer Membrane Proteins and Lipopolysaccharides for the Sensitivity of Escherichia coli to Antimicrobial Peptides. Front Microbiol 9:2153. doi:10.3389/fmicb.2018.02153

European Union Regulations Commission (2010) Commission Regulation (EU) No 37/2010 of 22 December 2009 on pharmacologically active substances and their classification regarding maximum residue limits in foodstuffs of animal origin. Off J Eur Union 53(15):1-72

FAO-WHO (2018) Maximum Residue Limits (MRLs) and Risk Management Recommendations (RMRs) for Residues of Veterinary Drugs in Foods CX/MRL (2-2018). Codex Alimentarius, International Food Standards, Rome, Italy

Finlayson GD, Schiele B, Crowley JL Comprehensive colour image normalization. In, Berlin, Heidelberg, 1998. Computer Vision — ECCV'98. Springer Berlin Heidelberg, p 475-490

Founou LL, Founou RC, Essack SY (2016) Antibiotic Resistance in the Food Chain: A Developing Country-Perspective. Front Microbiol 7:1881. doi:10.3389/fmicb.2016.01881

Galili T (2015) dendextend: an R package for visualizing, adjusting and comparing trees of hierarchical clustering. Bioinformatics 31(22):3718-20. doi:10.1093/bioinformatics/btv428

Grennfelt P, Engleryd A, Forsius M, Hov Ø, Rodhe H, Cowling E (2020) Acid rain and air pollution: 50 years of progress in environmental science and policy. Ambio 49(4):849-864. doi:10.1007/s13280-019-01244-4

Guobiao standards (2019) National food safety standard—Maximum residue limits for veterinary drugs in foods (translated from Mandarin). In: Ministry of Agriculture and Rural Affairs of the People's Republic of China, National Health Commission of the People's Republic of China, State Administration for Market Regulation, (ed) GB 31650—2019.

Hassan MM, El Zowalaty ME, Lundkvist Å, Järhult JD, Khan Nayem MR, Tanzin AZ, Badsha MR, Khan SA, Ashour HM (2021) Residual antimicrobial agents in food originating from animals. Trends Food Sci Technol 111:141-150. doi:10.1016/j.tifs.2021.01.075

Hobbs EC, Yin X, Paul BJ, Astarita JL, Storz G (2012) Conserved small protein associates with the multidrug efflux pump AcrB and differentially affects antibiotic resistance. Proc Natl Acad Sci U S A 109(41):16696-701. doi:10.1073/pnas.1210093109

Hua Yan Water (2021) Ex-factory water report (translated from Mandarin). https://www.heisino.com/monitoring.aspx?nid=12. Accessed 30 June 2020

Inkscape Project (2020) Inkscape. 0.92.5 edn

Jerome M (2016) A generic webcam image acquisition plugin for ImageJ

Jindal S, Yang L, Day PJ, Kell DB (2019) Involvement of multiple influx and efflux transporters in the accumulation of cationic fluorescent dyes by Escherichia coli. BMC Microbiol 19(1):195. doi:10.1186/s12866-019-1561-0

Kay S, Zhao B, Sui D (2015) Can Social Media Clear the Air? A Case Study of the Air Pollution Problem in Chinese Cities. Prof Geogr 67:351-363

Kern B, Leiser OP, Misra R (2019) Suppressor Mutations in degS Overcome the Acute Temperature-Sensitive Phenotype of ΔdegP and ΔdegP Δtol-pal Mutants of Escherichia coli. J Bacteriol 201(11). doi:10.1128/jb.00742-18

Kim HJ, Jang S (2018) Optimization of a resazurin-based microplate assay for large-scale compound screenings against Klebsiella pneumoniae. 3 Biotech 8(1):3. doi:10.1007/s13205-017-1034-9

Li H, Durbin R (2009) Fast and accurate short read alignment with Burrows-Wheeler transform. Bioinformatics 25(14):1754-60. doi:10.1093/bioinformatics/btp324

Li H, Handsaker B, Wysoker A, Fennell T, Ruan J, Homer N, Marth G, Abecasis G, Durbin R (2009) The Sequence Alignment/Map format and SAMtools. Bioinformatics 25(16):2078-9. doi:10.1093/bioinformatics/btp352

Li N, Ho KWK, Ying GG, Deng WJ (2017) Veterinary antibiotics in food, drinking water, and the urine of preschool children in Hong Kong. Environ Int 108:246-252. doi:10.1016/j.envint.2017.08.014

Linsen SEV (2020) Uses for a microbial culture reaction well, multiwell plate, culture bed, and method for detecting biological activity (translated from Mandarin). China Patent

Linsen SEV (2021) Antibiotic residues in the environment: a table, an index and some reflections. Figshare

Liu A, Tran L, Becket E, Lee K, Chinn L, Park E, Tran K, Miller JH (2010) Antibiotic sensitivity profiles determined with an Escherichia coli gene knockout collection: generating an antibiotic bar code. Antimicrob Agents Chemother 54(4):1393-403. doi:10.1128/aac.00906-09

Liu G, Olsen JE, Thomsen LE (2019) Identification of Genes Essential for Antibiotic-Induced Up-Regulation of Plasmid-Transfer-Genes in Cephalosporin Resistant Escherichia coli. Front Microbiol 10:2203. doi:10.3389/fmicb.2019.02203

Llor C, Bjerrum L (2014) Antimicrobial resistance: risk associated with antibiotic overuse and initiatives to reduce the problem. Ther Adv Drug Saf 5(6):229-41. doi:10.1177/2042098614554919

Martinez JL (2009) Environmental pollution by antibiotics and by antibiotic resistance determinants. Environ Pollut 157(11):2893-902. doi:10.1016/j.envpol.2009.05.051

Mason KM, Munson RS, Jr., Bakaletz LO (2005) A mutation in the sap operon attenuates survival of nontypeable Haemophilus influenzae in a chinchilla model of otitis media. Infect Immun 73(1):599-608. doi:10.1128/iai.73.1.599-608.2005

Mitosch K, Rieckh G, Bollenbach T (2017) Noisy Response to Antibiotic Stress Predicts Subsequent Single-Cell Survival in an Acidic Environment. Cell Syst 4(4):393-403.e5. doi:10.1016/j.cels.2017.03.001

Morè N, Martorana AM, Biboy J, Otten C, Winkle M, Serrano CKG, Montón Silva A, Atkinson L, Yau H, Breukink E, den Blaauwen T, Vollmer W, Polissi A (2019) Peptidoglycan Remodeling Enables Escherichia coli To Survive Severe Outer Membrane Assembly Defect. mBio 10(1). doi:10.1128/mBio.02729-18

Mulani MS, Kamble EE, Kumkar SN, Tawre MS, Pardesi KR (2019) Emerging Strategies to Combat ESKAPE Pathogens in the Era of Antimicrobial Resistance: A Review. Front Microbiol 10:539. doi:10.3389/fmicb.2019.00539

Munteanu FD, Titoiu AM, Marty JL, Vasilescu A (2018) Detection of Antibiotics and Evaluation of Antibacterial Activity with Screen-Printed Electrodes. Sensors 18(3). doi:10.3390/s18030901

Nahrstedt H, Meinhardt F (2004) Structural and functional characterization of the Bacillus megaterium uvrBA locus and generation of UV-sensitive mutants. Appl Microbiol Biotechnol 65(2):193-9. doi:10.1007/s00253-004-1572-z

Navrátilová P (2008) Screening methods used for the detection of veterinary drug residues in raw cow milk a review. Czech J Food Sci 26(6):393-401

Nolivos S, Cayron J, Dedieu A, Page A, Delolme F, Lesterlin C (2019) Role of AcrAB-TolC multidrug efflux pump in drug-resistance acquisition by plasmid transfer. Science 364(6442):778-782. doi:10.1126/science.aav6390

Nüesch-Inderbinen M, Treier A, Zurfluh K, Stephan R (2019) Raw meat-based diets for companion animals: a potential source of transmission of pathogenic and antimicrobial-resistant Enterobacteriaceae. R Soc Open Sci 6(10):191170. doi:10.1098/rsos.191170

O'Neill J (2014) Antimicrobial resistance : tackling a crisis for the health and wealth of nations

R. Team (2014) R: A language and environment for statistical computing. MSOR connect

Raetz CR, Whitfield C (2002) Lipopolysaccharide endotoxins. Annu Rev Biochem 71:635-700. doi:10.1146/annurev.biochem.71.110601.135414

Reygaert WC (2018) An overview of the antimicrobial resistance mechanisms of bacteria. AIMS Microbiol 4(3):482-501. doi:10.3934/microbiol.2018.3.482

Rodriguez-Mozaz S, Vaz-Moreira I, Varela Della Giustina S, Llorca M, Barceló D, Schubert S, Berendonk TU, Michael-Kordatou I, Fatta-Kassinos D, Martinez JL, Elpers C, Henriques I, Jaeger T, Schwartz T, Paulshus E, O'Sullivan K, Pärnänen KMM, Virta M, Do TT, Walsh F, Manaia CM (2020) Antibiotic residues in final effluents of European wastewater treatment plants and their impact on the aquatic environment. Environ Int 140:105733. doi:10.1016/j.envint.2020.105733

Rueden CT, Schindelin J, Hiner MC, DeZonia BE, Walter AE, Arena ET, Eliceiri KW (2017) ImageJ2: ImageJ for the next generation of scientific image data. BMC Bioinform 18(1):529. doi:10.1186/s12859-017-1934-z

Schoenmakers K (2020) How China is getting its farmers to kick their antibiotics habit. Nature 586:S60-S62

Shepherd CJ, Jackson AJ (2013) Global fishmeal and fish-oil supply: inputs, outputs and markets. J Fish Biol 83(4):1046-66. doi:10.1111/jfb.12224

Stubbings W, Bostock J, Ingham E, Chopra I (2005) Deletion of the multiple-drug efflux pump AcrAB in Escherichia coli prolongs the postantibiotic effect. Antimicrob Agents Chemother 49(3):1206-8. doi:10.1128/aac.49.3.1206-1208.2005

Sugiyama Y, Nakamura A, Matsumoto M, Kanbe A, Sakanaka M, Higashi K, Igarashi K, Katayama T, Suzuki H, Kurihara S (2016) A Novel Putrescine Exporter SapBCDF of Escherichia coli. J Biol Chem 291(51):26343-26351. doi:10.1074/jbc.M116.762450

Szczepaniak J, Press C, Kleanthous C (2020) The multifarious roles of Tol-Pal in Gram-negative bacteria. FEMS Microbiol Rev 44(4):490-506. doi:10.1093/femsre/fuaa018

Taylor PL, Blakely KM, de Leon GP, Walker JR, McArthur F, Evdokimova E, Zhang K, Valvano MA, Wright GD, Junop MS (2008) Structure and function of sedoheptulose-7-phosphate isomerase, a critical enzyme for lipopolysaccharide biosynthesis and a target for antibiotic adjuvants. J Biol Chem 283(5):2835-45. doi:10.1074/jbc.M706163200

The Document Foundation (2020) LibreOffice Calc. 2020 (6.3.6) edn

Van Boeckel TP, Brower C, Gilbert M, Grenfell BT, Levin SA, Robinson TP, Teillant A, Laxminarayan R (2015) Global trends in antimicrobial use in food animals. Proc Natl Acad Sci U S A 112(18):5649-54. doi:10.1073/pnas.1503141112

Van der Auwera GA, Carneiro MO, Hartl C, Poplin R, Del Angel G, Levy-Moonshine A, Jordan T, Shakir K, Roazen D, Thibault J, Banks E, Garimella KV, Altshuler D, Gabriel S, DePristo MA (2013) From FastQ data to high confidence variant calls: the Genome Analysis Toolkit best practices pipeline. Curr Protoc Bioinform 43(1110):11.10.1-11.10.33. doi:10.1002/0471250953.bi1110s43

Van TTH, Yidana Z, Smooker PM, Coloe PJ (2020) Antibiotic use in food animals worldwide, with a focus on Africa: Pluses and minuses. J Glob Antimicrob Resist 20:170-177. doi:10.1016/j.jgar.2019.07.031

Wang H, Ren L, Yu X, Hu J, Chen Y, He G, Jiang Q (2017) Antibiotic residues in meat, milk and aquatic products in Shanghai and human exposure assessment. Food Control 80:217-225

Wang H, Tang C, Yang J, Wang N, Jiang F, Xia Q, He G, Chen Y, Jiang Q (2018) Predictors of urinary antibiotics in children of Shanghai and health risk assessment. Environ Int 121(Pt 1):507-514. doi:10.1016/j.envint.2018.09.032

Warnes MGR, Bolker B, Bonebakker L, Gentleman R, Huber W (2016) Package 'gplots'. Various R programming tools for plotting data

Waternet (2021) Waterkwaliteit drinkwater Amsterdam. https://www.waternet.nl/service-en-contact/drinkwater/waterkwaliteit/. Accessed 30 June 2020

Werner J, Misra R (2005) YaeT (Omp85) affects the assembly of lipid-dependent and lipid-independent outer membrane proteins of Escherichia coli. Mol Microbiol 57(5):1450-9. doi:10.1111/j.1365-2958.2005.04775.x

Yajko DM, Madej JJ, Lancaster MV, Sanders CA, Cawthon VL, Gee B, Babst A, Hadley WK (1995) Colorimetric method for determining MICs of antimicrobial agents for Mycobacterium tuberculosis. J Clin Microbiol 33(9):2324-7. doi:10.1128/jcm.33.9.2324-2327.1995

Yethon JA, Vinogradov E, Perry MB, Whitfield C (2000) Mutation of the lipopolysaccharide core glycosyltransferase encoded by waaG destabilizes the outer membrane of Escherichia coli by interfering with core phosphorylation. J Bacteriol 182(19):5620-3. doi:10.1128/jb.182.19.5620-5623.2000

Figures

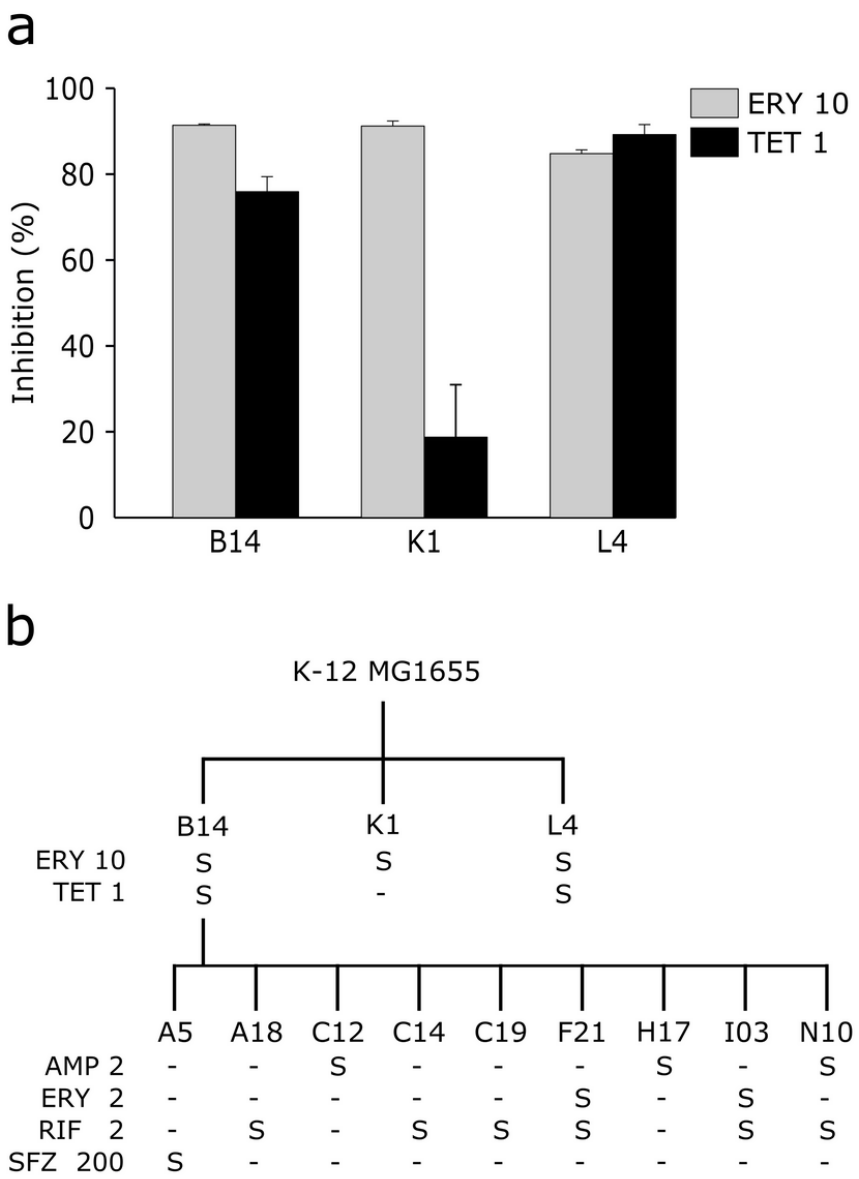

Figure 1

Initial characterization of ABSBs. (a) Growth inhibition by the indicated antibiotics (μg/mL) was determined for MG1655 and the first-generation ABSBs using an OD600 end-point assay in LB medium at 11 hours. Strains show 80% inhibition against at least one of the antibiotics used. (b) Lineage tree of ABSBs derived from MG1655 in this study. S indicates observed sensitivity to the given antibiotic concentrations during the initial and second screen.

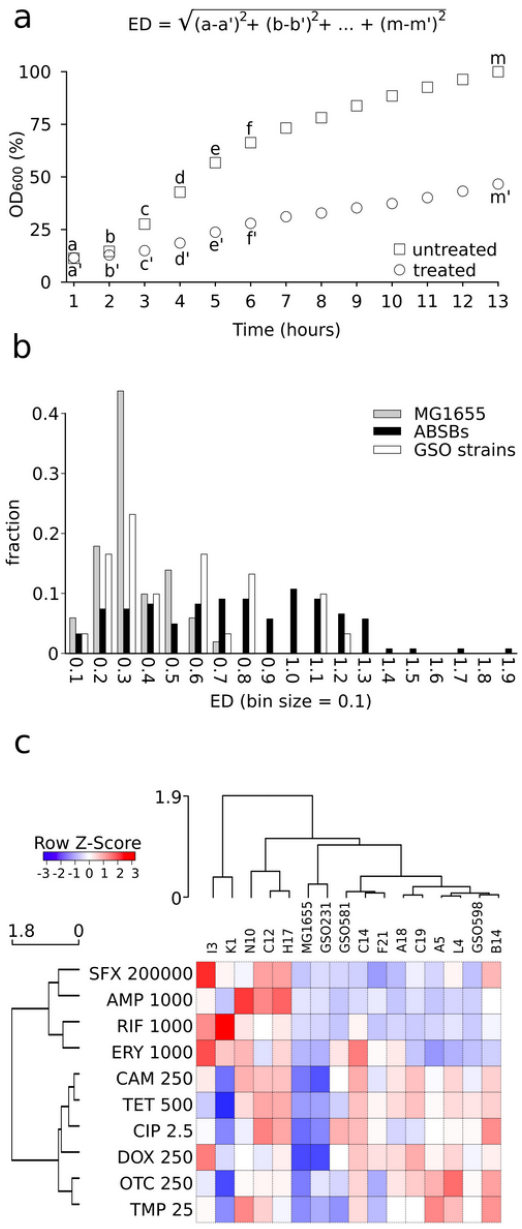

Figure 2

Response of ABSBs and reference strains to antibiotics using OD-based ARED. (a) A theoretical example of OD-based ARED showing growth inhibition of an antibiotic-treated strain compared to the untreated strain. The highest OD600 value of the non-treated sample is set to 100% and the ED is subsequently calculated with the percentage-transformed OD600 values according to the formula. (b) ED value distribution of our complete OD600 dataset obtained from MG1655, GSO strains and the 12 ABSBs grown in presence of antibiotics. (c) Hierarchical clustering of correlations between ED values of the indicated strains and antibiotics. Antibiotics concentrations shown in ng/mL, axes left and above the dendrograms indicate node height. The underlying data for these figures is shown in Table 3.

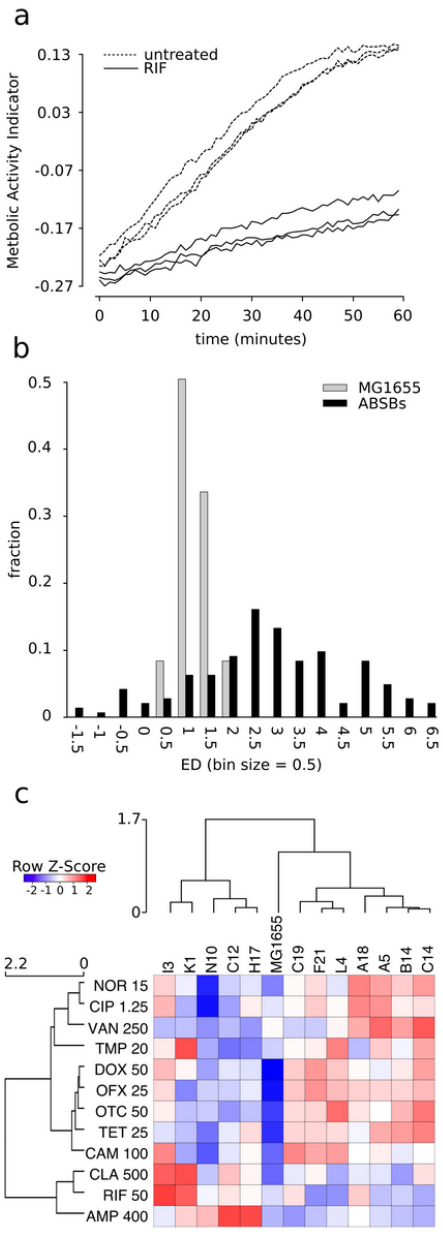

Figure 3

Antibiotic sensitivity of ABSBs determined by resazurin-based ARED. (a) Metabolic Activity Indicator changes over time in resazurin-based ARED with K1 incubated with or without 50 ng/mL RIF. (b) Distribution of ED values of MG1655 and ABSBs. (c) Hierarchical clustering of correlations between ED values of indicated strains. Antibiotics concentrations shown in ng/mL, axes left and above the dendrograms indicate node height. The underlying data for these figures is shown in Table 4.

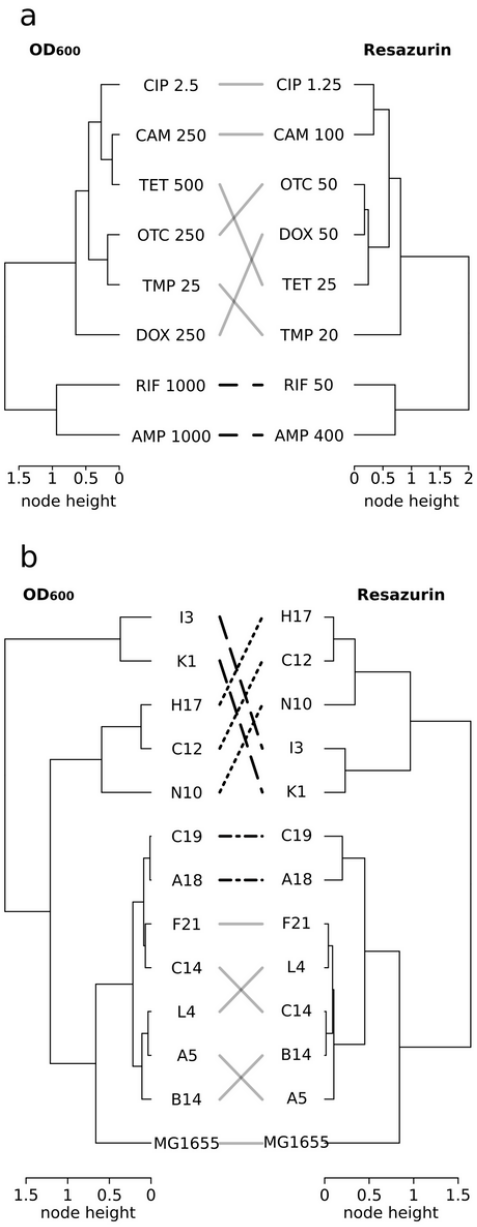

Figure 4

Alignment of OD-based ARED and resazurin-based ARED dendrograms. (a) Dendrograms of the antibiotic types alignment displays a correlation of 0.76 (P value alignment is 0.065). (b) Dendrograms of strains (MG1655 and all ABSBs) show a correlation value of 0.8 (P value alignment is 0). Dashed line types display subtrees that branch identically in both dendrograms, with a separate pattern for each of these subtrees. Grey lines indicate a difference in subtree branching.

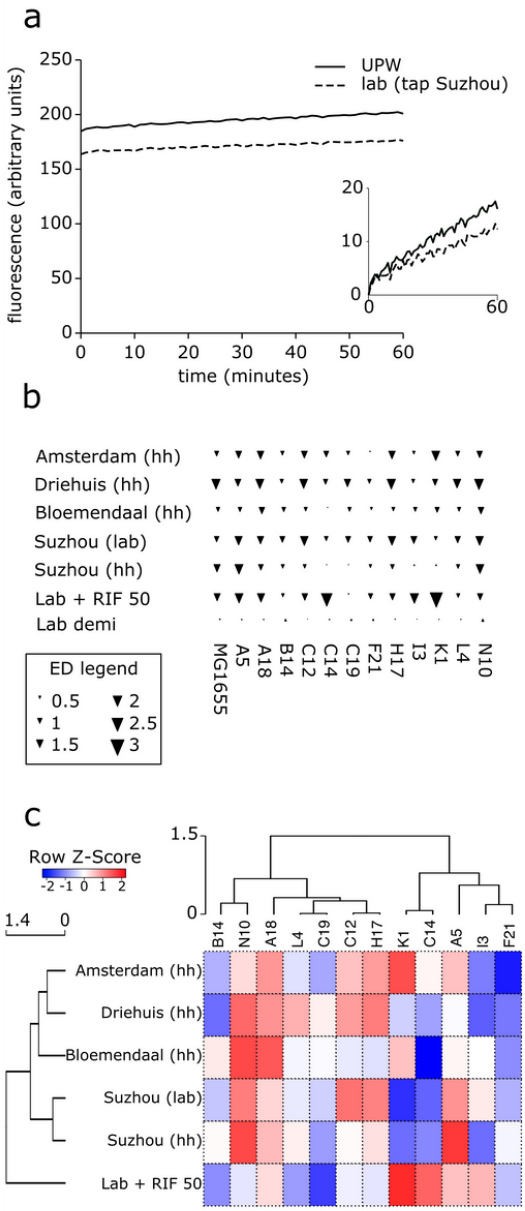

Figure 5

Resazurin-based ARED applied to tap water samples from different geographical locations. (a) Resazurin reduction in tap water and UPW, as measured by fluorescence (excitation 560 nm, emission 590 nm). The inset presents the absolute intensity increase since t=0, with the signal accumulation in UPW stronger and more rapid. (b) ED values (indicated by differently sized triangles) for tap water from three households (hh) in the Netherlands (Amsterdam, Driehuis and Bloemendaal), a Suzhou household and our laboratory (lab) in Suzhou, as well as demineralized (demi) lab water and RIF-spiked (50 ng/mL) lab water. (c) Hierarchical clustering of correlations between ED values of ABSBs from which the MG1655 ED value was subtracted. Axes left and above the dendrograms indicate node heights.

Supplementary Files

This is a list of supplementary files associated with this preprint. Click to download.

- GAbstractsmall.png
- ShiAREDbiosensorsSI.xlsx